J|A|C|S
ARTICLES

Published on Web 05/20/2009

Bridgehead Lithiation-Substitution of Bridged Ketones, Lactones, Lactams, and Imides: Experimental Observations and Computational Insights

Christopher J. Hayes,* Nigel S. Simpkins,*,† Douglas T. Kirk, Lee Mitchell, Jerome Baudoux, Alexander J. Blake, and Claire Wilson

School of Chemistry, The University of Nottingham, University Park, Nottingham, NG7 2RD United Kingdom

Received February 10, 2009; E-mail: n.simpkins@bham.ac.uk

Abstract: The viability of bridgehead lithiation-substitution of bridged carbonyl compounds has been tested in the laboratory, and the results were rationalized with the aid of a computational study. Lithiation-substitution was found to be possible for ketones, lactones, lactams, and imides having small bridges, including examples having [3.2.1], [3.2.2], [3.3.1], [4.2.1], and [4.3.1] skeletons. Smaller systems, where the sum of the bridging atoms (*S*) was 5, for example [2.2.1] or [3.1.1] ketones or [2.2.1] lactams, did not undergo controlled bridgehead substitution. Ketones or lactams having a [2.2.2] structure also did not give bridgehead substitution. B3LYP calculations accurately predict this behavior with negative ΔE_{rxn} values being calculated for the successful deprotonations and positive ΔE_{rxn} values being calculated for the unsuccessful ones. NBO calculations were also performed on the anionic deprotonated species, and these show that some structures are best represented as bridgehead enolates and some are best represented as α-keto carbanions.

Introduction

The metalation of carbonyl compounds at bridgehead positions, to form intermediates that can be described as "bridgehead enolates", is expected to be more difficult than the enolization of "normal" cyclic or acyclic analogues. Both the stereoelectronic aspects of the deprotonation process[1] and the degree of planarised enolate character[2] will be modified due to the constraints placed on the system by the bridged structure. This issue is expected to be particularly acute for compounds having only small bridges where the conventional planar enolate form of the resulting anion would contravene Bredt's rule.[3]

The issues of bridgehead enol and enolate formation, and the parallels with bridgehead alkene stability, have long been recognized, and early work is described in a review by Shea.[4] We became interested in the metalation of bridged systems through our work on the applications of chiral lithium amides bases,[5] and this led us to review the literature concerning the formation and reactions of bridgehead metal enolates. Much of the early work involved the study of H−D exchange of bridged ketones under protic conditions, and we identified only a limited number of examples where enolate generation and substitution (especially C−C bond formation) had been conducted under aprotic conditions using bases such as LDA or LHMDS, etc. (*vide infra*). This was particularly true for systems having only small bridges (i.e., where the total number of bridging atoms (*S*) is only 5−7)[6] where the viability of bridgehead enolate formation and substitution appeared most doubtful.

Scheme 1

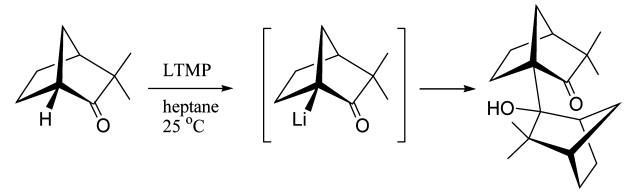

1 **2** **3** 90%

Herein we describe our work in this area, in which we have combined experimental testing of bridgehead metalations of a range of carbonyl compounds, including ketones, lactones, lactams and imides, with theoretical calculations, in order to try and address key issues.[7,8] These include: (i) clarification of the combinations of bridge sizes and carbonyl functions (and their positioning), which enable effective metalation-substitution; (ii) enantioselective bridgehead metalation of certain substrates

† Current address: School of Chemistry, The University of Birmingham, Edgbaston, Birmingham, B15 2TT, U.K.

(1) For leading references, see: Behnam, S. M.; Behnam, S. E.; Ando, K.; Green, N. S.; Houk, K. J. *J. Org. Chem.* **2000**, *65*, 8970.
(2) Seebach, D. *Angew. Chem., Int. Ed.* **1988**, *27*, 1624.
(3) For a review, see: (a) Warner, P. M. *Chem. Rev.* **1989**, *89*, 1067. For more recent synthetic work aimed at bridgehead alkenes, see: (b) Roach, P. Warmuth, R. *Angew. Chem. Int. Ed.* **2003**, *42*, 3039. (c) Mehta, G. Kumaran, R. S. *Chem. Commun.* **2002**, 1456. (d) Bear, B. R. Sparks, S. M. Shea, K. J. *Angew. Chem., Int. Ed.* **2001**, *40*, 821. See also ref 4.
(4) Shea, K. J. *Tetrahedron* **1980**, *36*, 1683.
(5) For our most recent contributions, see: (a) Rodeschini, V.; Simpkins, N. S.; Wilson, C. *J. Org. Chem.* **2007**, *72*, 4265. (b) Rodeschini, V.; Simpkins, N. S.; Zhang, Z. *Org. Synth.* **2007**, *84*, 306. (c) Butler, B.; Schultz, T.; Simpkins, N. S. *Chem. Comm.* **2006**, 3634.
(6) Werstiuk, N. H. *Tetrahedron* **1983**, *39*, 205.
(7) Blake, A. J.; Giblin, G. M. P.; Kirk, D. T.; Simpkins, N. S.; Wilson, C. *Chem. Commun.* **2001**, 2668.
(8) Giblin, G. M. P.; Kirk, D. T.; Mitchell, L.; Simpkins, N. S. *Org. Lett.* **2003**, *5*, 1673.

10.1021/ja9009875 CCC: $40.75

using chiral lithium amide bases; (iii) probing enolate vs carbanionic character in the intermediates, and development of computational methods as useful tools for better understanding and predicting bridgehead metalation.

Results and Discussion

(i) Bridged Ketones. Our interest in this area was originally stimulated by a report from 1988 describing a selection of unconventional metalations using lithium dialkylamide bases, including bridgehead lithiation of camphenilone **1** using lithium tetramethylpiperidide (LTMP), Scheme 1.[9]

The reaction gave "aldol dimer" **3** as the sole product in high yield, via a bridgehead metalated intermediate that the authors formulated as **2**. Although this result provided evidence of the viability of bridgehead metalation, even in a system with a low *S* value (5), a later report by Spitz and Eaton referred to their inability to "trap the putative intermediate pseudoenolates", "despite intense efforts".[10]

A more in depth survey of the literature revealed several other significant results, including the conversion of benzannulated 7-oxabicyclo[2.2.1]heptanone **4** (R = H) into the bridgehead silylated derivative **4** (R = $SiMe_3$), using LTMP with an *in situ* Me_3SiCl quench.[11] In the absence of a quench, the ketone underwent the same type of aldol-type process shown in Scheme 1.

In syntheses of patchouli alcohol and seychellene, Yamada had demonstrated the bridgehead methylation and hydroxylation of ketone **5** (R = H), essentially a [2.2.2] bridged system with an additional ring.[12] The same group described the synthesis of enol silane **6**, from the corresponding ketone (LDA, DME, −20 °C), and described it as having reduced carbon−carbon double bond character compared with a standard enol silane.[13]

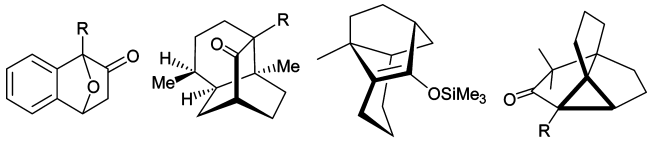

4 **5** **6** **7**

Finally, a synthesis of modhephene incorporated the bridgehead carboxymethylation of ketone **7** (R = H) to give the corresponding ketoester **7** (R = CO_2Me).[14] As with the other systems mentioned, this ketone has special features that preclude too much generalization about the viability of bridgehead substitution in ketones having small bridges.

On the other hand, there are a reasonable number of examples of bridgehead substitutions of ketones having larger rings (say $S > 8$). Many of these have been carried out as part of natural product syntheses, and so the structures of the ketones are diverse, often bearing substituents and functionality unique to the intended target. Examples of substrates usefully employed include **8**−**12**.[15−19]

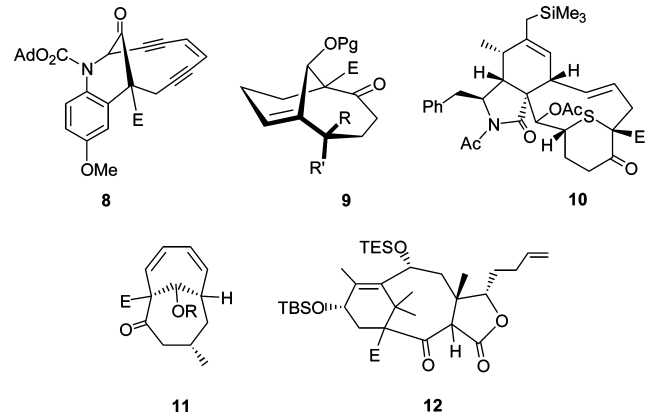

8 **9** **10**

11 **12**

Issues of regiochemistry arise in each of these, and in each case effective substitution could be carried out at the position indicated by an E. Several of the results are especially remarkable, since the bridgehead metalation-electrophilic substitution occurs despite the possibility of the formation of a "normal" enolate by deprotonation at the alternative α-position. It is clear that, in a number of cases, such ketones are predisposed to bridgehead metalation for either stereoelectronic reasons (i.e., perfect alignment of the hydrogen to be abstracted), or due to special stabilizing features in the bridgehead "enolate" itself—for example, extended conjugation (as in **11**).[18]

With this background, we set out with the intention of testing a range of bicyclic ketones for their bridgehead lithiation potential, focusing on simple frameworks where $S = 5-7$, and using chlorotrimethylsilane as electrophilic quenching agent.

We quickly verified the difficulties in attempting to trap the putative lithiated intermediate corresponding to **2** and were unable, under a wide variety of basic conditions, to isolate products other than **3**. Camphenilone appears to represent a borderline case, where metalation, although viable, does not enable any useful substitution.

We next examined a raft of related ketones, including examples from the [3.1.1], [2.2.2], [3.3.1], [3.2.1] and [3.2.2] families, **13**−**16**. These compounds were either commercially available (**15**) or were easily prepared by α-gem-dimethylation of the known parent bicyclic ketones.

In the cases of **13**−**15**, we were not able to affect bridgehead lithiation under a range of conditions, using either LDA or LTMP as base. In the absence of Me_3SiCl we saw no evidence for self-addition, analogous to Scheme 1. In the presence of a silyl quench we observed either no reaction or, in the case of attempted lithiation of **15** with LDA, only traces of undesired product arising from ketone reduction-silylation.

This behavior was in sharp contrast with that of ketones **16** and **17**, which could be converted into the corresponding α-silylketones **18** (52−60% with either LDA-LiCl or LTMP) and **19** (70% with LTMP-LiCl) respectively, by addition of a

(9) Shiner, C. S.; Berks, A. H.; Fisher, A. M. *J. Am. Chem. Soc.* **1988**, *110*, 957.
(10) Spitz, U. P.; Eaton, P. E. *Angew. Chem., Int. Ed. Engl.* **1994**, *33*, 2220.
(11) Mirsadeghi, S.; Rickborn, B. *J. Org. Chem.* **1986**, *51*, 986.
(12) Yamada, K.; Kyotani, Y.; Manabe, S.; Suzuki, M. *Tetrahedron* **1979**, *35*, 293. See also: (a) Niwa, H.; Wakamatsu, K.; Hida, T.; Niiyama, K.; Kigoshi, H.; Yamada, M.; Nagase, H.; Suzuki, M.; Yamada, K. *J. Am. Chem. Soc.* **1984**, *106*, 4547.
(13) Wakamatsu, K.; Tan, H.; Ban, N.; Uchiyama, N.; Niwa, H.; Yamada, K. *Chem. Lett.* **1987**, 121.
(14) Wrobel, J.; Takahashi, K.; Honkan, V.; Lannoye, G.; Cook, J. M.; Bertz, S. H. *J. Org. Chem.* **1983**, *48*, 139.
(15) Magnus, P.; Eisenbeis, S. A.; Fairhurst, R. A.; Iliadis, T.; Magnus, N. A.; Parry, D. *J. Am. Chem. Soc.* **1997**, *119*, 5591.
(16) Clive, D. L. J.; Sun, S.; Gagliardini, V.; Sano, M. K. *Tetrahedron Lett.* **2000**, *41*, 6259.
(17) Vedejs, E.; Rodgers, J. D.; Wittenberger, S. J. *J. Am. Chem. Soc.* **1988**, *110*, 4822.
(18) Rigby, J. H.; Moore, T. L. *J. Org. Chem.* **1990**, *55*, 2959.
(19) Holton, R. A. *J. Am. Chem. Soc.* **1994**, *116*, 1597. See also: Wender, P. A.; Mucciaro, T. P. *J. Am. Chem. Soc.* **1992**, *114*, 5878.

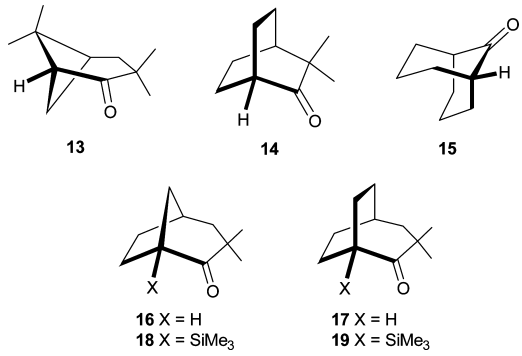

lithium amide base (2 equivalents) to a mixture of the ketone and Me_3SiCl in THF at low temperature.

We spent considerable time studying the substitution chemistry of the two [4.2.1] systems, **20** and **21**, which were easily prepared from cyclooctatetraene.[20] The unsaturated compound, bicyclo[4.2.1]nona-2,4,7-trien-9-one **21**, had previously been reported to undergo self-addition on treatment with base (KHMDS).[21] We also observed this behavior, using LTMP as base, and isolated the addition product **22** in an improved yield compared to that described previously, Scheme 2.

Our next step was to add a solution of ketone **21** to an excess of LDA-LiCl in the presence of Me_3SiCl at −105 °C, which provided an inseparable mixture of the *bis*-silylated ketones **23** and **24** in a 1:4 ratio and in 63% yield. A similar result was obtained using LTMP (71% yield), Scheme 3.

The formation of the tetracyclic ketone **24** was unexpected and was confirmed following a single crystal X-ray structure determination, Figure 1.

This product is the result of double bridgehead substitution followed by a transannular Diels−Alder reaction, the latter process being precedented for this type of system.[22] Very similar results were seen by using LTMP as the base. We observed no monosilylated ketone corresponding to **24**, which points to its formation purely via **23**. An alternative mechanism involving anion initiated cycloaddition of **21** followed by *bis*-silylation appears to be ruled out following further experiments described below.

By changing the mode of reagent mixing and limiting the amount of base and Me_3SiCl employed we hoped to minimize formation of the unwanted *bis*-silyl compounds **23** and **24**. This proved to be the case; addition of LDA-LiCl (1.1 equiv) to a mixture of ketone and Me_3SiCl (i.e., inverse addition) at −105 °C, gave the mono silylated ketone **25** in 38% yield, accompanied by a mixture of **23** and **24** in 17% yield, Scheme 4.

Next we attempted the asymmetric deprotonation of **21** by employing chiral base (*R*,*R*)-**26**.[23] By using the inverse addition protocol with (*R*,*R*)-**26** at −105 °C we obtained mono silylated ketone (−)-**25** in 76% yield, with an excellent e.e. of 98%, in addition to *bis*-silylated ketones **23/24** in 23% yield. Conducting the reaction at −78 °C led to a lower yield of (−)-**25** (46%) and slightly lower enantiomeric excess (92%). The absolute configuration of (−)-**25** was determined by single crystal X-ray structure determination (Figure 2).

Scheme 2

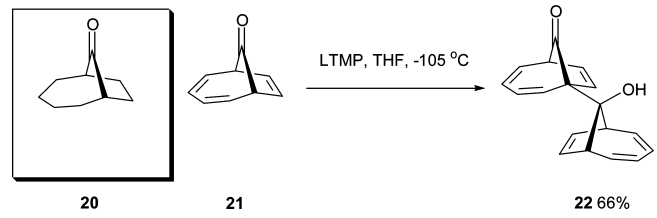

Scheme 3

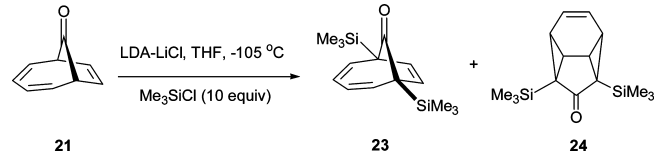

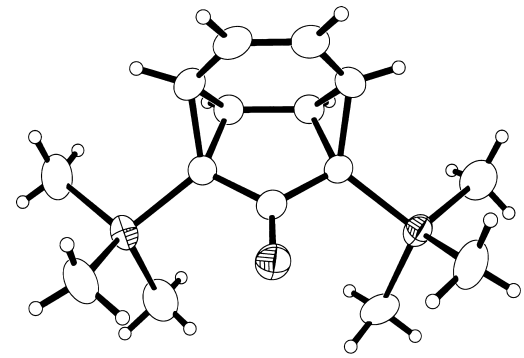

Figure 1. X-ray structure of **24**.

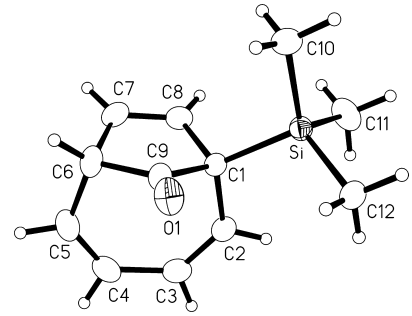

Figure 2. X-ray structure of (−)-**25**.

The monosilylated ketone **25** was never accompanied by any of the monosilylated tetracycle corresponding to **24**, and even heating **25** in an effort to induce some level of cyclization resulted only in recovery of starting ketone, or eventual decomposition at higher temperatures. Thus it appears that disilylation of starting diketone to give **23** is a prerequisite for the generation of **24**.

Somewhat analogous bridgehead silylation chemistry was established for the saturated bicyclic ketone **20**. Thus, attempted external quenching reactions were unproductive, or gave products from self-addition, similar to **22**, whereas the inverse addition protocol readily provided racemic silylketone **27** using LDA, or enantiomerically enriched **27** by use of the chiral base **26**, Scheme 5.

Surprisingly in these reactions we did not observe the formation of doubly silylated products-even if we switched back to adding the ketone to excess base-Me_3SiCl. The reasons for this striking difference are unclear and we did not make a

(20) Antkowiak, T. A.; Sanders, D. C.; Trimitsis, G. B.; Press, J. B.; Shechter, H. *J. Am. Chem. Soc.* **1972**, *94*, 5366.
(21) Feldman, K. S.; Come, J. H.; Kosmider, B. J.; Smith, P. M.; Rotella, D. P.; Wu, M.-J. *J. Org. Chem.* **1989**, *54*, 592.
(22) Miller, R. D.; Dolce, D. L. *Tetrahedron Lett.* **1977**, 3329.
(23) For reviews of chiral lithium amide base reactions, see: (a) O'Brien, P. *J. Chem. Soc., Perkin Trans. 1* **1998**, 1439. (b) Hodgson, D. M.; Stent, M. A. H. *Top. Organometallic Chem.* **2003**, *5*, 1.

Scheme 4

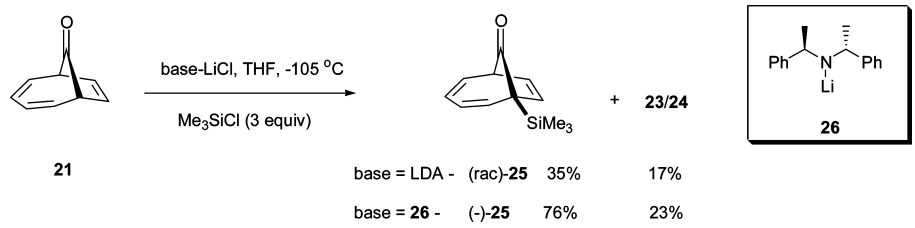

Scheme 5

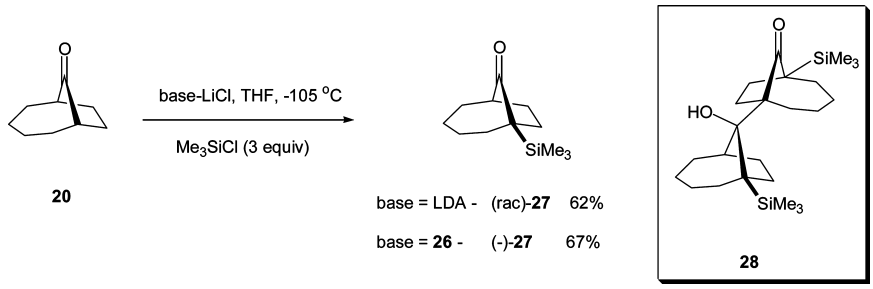

Scheme 6

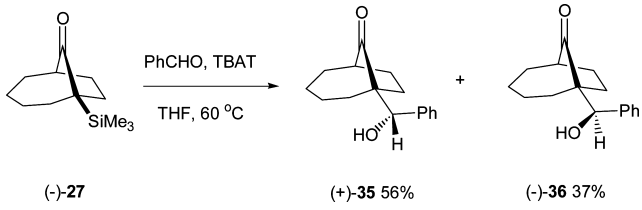

determined effort to doubly silylate **20**. Silylketone (−)-**27** was not readily amenable to ee determination, and so we established the level of asymmetric induction (*ca*. 92%) by hydrogenating a sample of (−)-**25** to enable correlation of the two series. This also established that the sense of deprotonation was the same in both cases.

Despite our failed attempts to effect external quench reactions with **20**, we wondered if the silylketones **25** and **27** might show improved behavior, the bulky trimethylsilyl substituent being a potential deterrent to self-addition. However, this proved not to be the case, and attempted substitution, using external quenching protocols led only to self-addition products such as **28**.

Since our efforts to introduce directly carbon bridgehead substituents had failed, we adopted an alternative indirect tactic that had proved effective in the past—namely *ipso*-substitution of a bridgehead silicon group under the influence of fluoride.[24] Thus, treatment of enantiomerically enriched (−)-**25** with tetrabutylammonium triphenyldifluorosilicate (TBAT),[25] in the presence of a small selection of electrophiles, resulted in the formation of bridgehead C-substituted products, Table 1.

The enantiomeric excess of the starting silane was maintained in the products, based on our analysis of the diastereomeric benzaldehyde aldol products **32**. Yields were modest for alkylation processes, with proto-desilylation being competitive, whereas aldol-type condensation proved much more efficient.

Reaction with Mander's reagent, methyl cyanoformate ($NCCO_2Me$), gave clean conversion to a bridgehead substituted product **34** lacking a bridging ketone function. The structure of this product was determined following an X-ray structure determination, Figure 3.

The structure confirmed that bridgehead carboxymethylation had indeed been achieved, but that concomitant cyanohydrin formation and acylation had also occurred. As far as we could ascertain, the cyanohydrin was formed with complete diastereocontrol, with *exo* attack of cyanide occurring to give only the isomer shown.

Similar fluoride mediated substitution was also shown to be possible, starting with the corresponding saturated ketosilane (−)-**27**, although this required slightly more forcing conditions, Scheme 6.

Table 1. Ipso-Substitution of (−)-**25** using TBAT

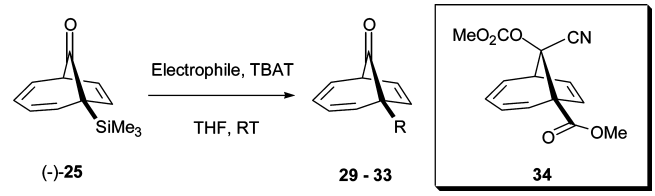

electrophile	product (R)	yield (%)
MeI	**29** (Me)	49
Allyl bromide	**30** (Allyl)	39
Benzyl bromide	**31** (Bn)	41
PhCHO	**32** (CH(OH)Ph)	72[a]
CyCHO	**33** (CH(OH)Cy)	78[b]

[a] ca. 3:2 ratio of diastereoisomers. [b] ca. 4:1 ratio of diastereoisomers (Cy = cyclohexyl).

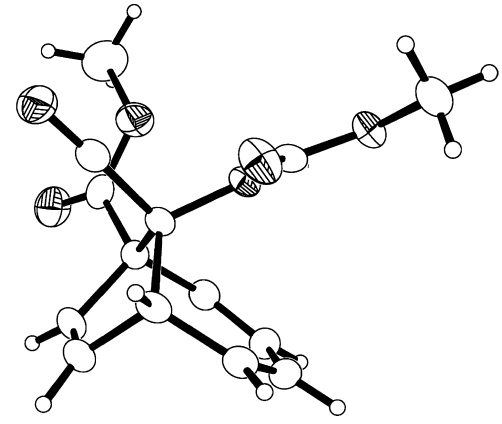

Figure 3. X-ray structure of **34**.

Thus, for effective reaction this system required warming to 60 °C, but then furnished the two diastereomeric "aldol" type products **35** and **36** in an excellent 93% combined yield. The relative configurations shown for these two adducts were assigned following X-ray analysis of the crystalline minor isomer (−)-**36**, Figure 4.

Both of the hydroxyketone products **35** and **36** were optically active and, based on the precedent established with the corresponding unsaturated adducts **32**, we presume that the stereochemical integrity of these systems is retained - although we have no evidence in this case. No further extension of this chemistry was carried out on silylketone (−)-**27** and we turned our attention to bridgehead lithiation of additional ketones.

A further system that proved amenable to study was the tricyclic ketone **37**, readily available by the [6 + 4] cycloaddition of tropone to cyclohexa-1,3-diene.[26] Silylation of this ketone using LTMP proved high-yielding, giving **38** in racemic form, Scheme 7.

Attempts to access this product in nonracemic form by deprotonation with either chiral base **26**, or the *bis*-lithium amide **39** were less satisfactory than with ketones **20** and **21**, particularly since we could not achieve complete enantiomer separations in our HPLC assay. Our preliminary studies appear to indicate very modest levels of asymmetric induction (ca. 20%) using base **26**, and higher selectivity (ca. 70%) with base **39** (albeit with a low chemical yield of 30%).

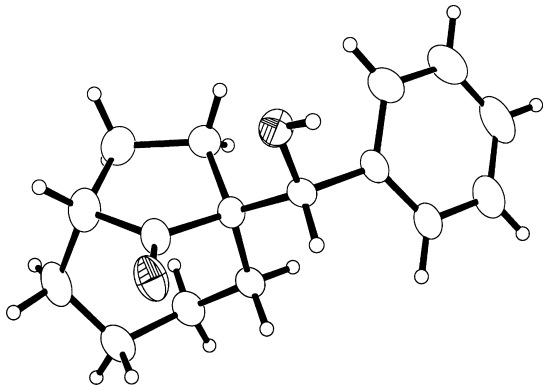

Figure 4. X-ray structure of (−)-**36**.

Scheme 7

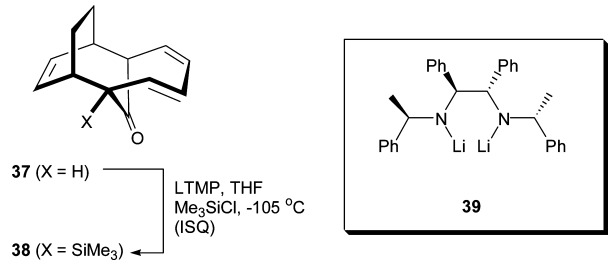

Scheme 8

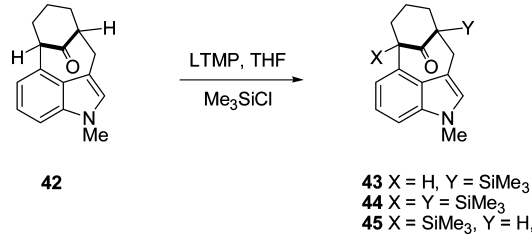

At this point our attention was drawn to the possibility of usefully employing bridgehead substitution in the context of natural product synthesis. Specifically, we became interested in the welwitindolinone alkaloids, which include *N*-methylwelwitindolinone C isothiocyanate (**40**), otherwise known as welwistatin, and welwitindolinone A (**41**).[27]

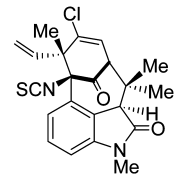

40 *N*-methylwelwitindolinone C isothiocyanate (welwistatin)

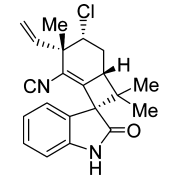

41 welwitindolinone A isonitrile

Welwistatin became the focus of our attention, in part due to its reported ability to reverse P-glycoprotein mediated multidrug resistance, and in 2005 we published a rather short access to a bridged ketoindole (**42**) that bears obvious resemblance to this natural product.[28] Since welwistatin displays a bridgehead substituent, in the form of an unusual isothiocyanate function, we naturally decided to probe the bridgehead substitution chemistry of this system, Scheme 8.

Initial studies using LDA as base proved unproductive, with only ketone reduction being observed when excess reagent was employed. In contrast, addition of one equivalent of LTMP to a mixture of ketone **42** and Me_3SiCl, initially at −78 °C, and then allowing the mixture to warm to room temperature, resulted in clean formation of the monosilylated product **43** in 54% yield. A similar procedure, using five equivalents of base led to the formation of the *bis*-silylated product **44** in 67% yield. Intermediate quantities of base simply resulted in mixtures of these two products, and we did not observe any of the regioisomeric silylated product **45**, which corresponds to the sense of substitution required for the natural product welwistatin.

Work in this area is ongoing within our group, particularly the use of **43** in further substitution reactions, the ipso-substitution of the silicon substituent in **44**, the use of alternative electrophilic quenches, and the use of equilibrating conditions to achieve the desired regiocontrol.

For completeness, it is worth also including mention at this point of another family of bridged ketonic substrates, which have been successfully employed in bridgehead substitution reactions. Thus, lithiation and prenylation of the *O*-methylated trione **46**, to give **47**, constituted a key step in our recently disclosed synthesis of the polyprenylated acylphloroglucinol natural product clusianone, Scheme 9.[29]

Full details of this chemistry will be described elsewhere but it is useful to note here that a number of such vinylogous ester systems related to **46** undergo rather efficient bridgehead

(24) Adams, D. J.; Blake, A. J.; Cooke, P. A.; Gill, C. D.; Simpkins, N. S. *Tetrahedron* **2002**, *58*, 4603.
(25) Pilcher, A. S.; Ammon, H. L.; Deshong, P. *J. Am. Chem. Soc.* **1995**, *117*, 5166.
(26) Takeshita, H.; Sugiyama, S.; Hatsui, T. *J. Chem. Soc., Perkin Trans. II* **1986**, 1491.
(27) Stratmann, K.; Moore, R. E.; Bonjouklian, R.; Deeter, J. B.; Patterson, G. M. L.; Shaffer, S.; Smith, C. D.; Smitka, T. A. *J. Am. Chem. Soc.* **1994**, *116*, 9935.
(28) Baudoux, J.; Blake, A. J.; Simpkins, N. S. *Org. Lett.* **2005**, *7*, 4087. For a review, see: Menendez, J. C. *Top. Het. Chem.* **2007**, *11*, 63.

Scheme 9

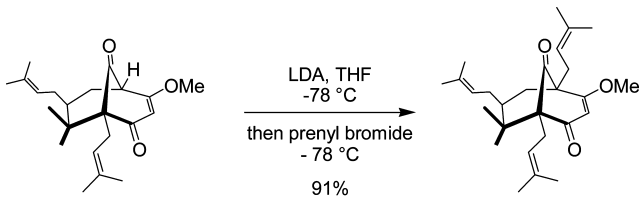

46 **47**

substitution—particularly direct *C*-substitution, in a regiocontrolled fashion.[30]

Finally, we also established that 1,3-diketone substrates may undergo bridgehead silylation without the need to *O*-alkylate the diketone enol function, Scheme 10.

Scheme 10

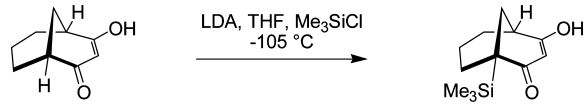

48 **49**

An excess of LDA-LiCl was added to a solution of the readily available [3.3.1]-dione **48** and Me_3SiCl, and after slow warming and standard workup gave the bridgehead silylated dione **49** in a modest yield. This reaction could involve the intermediacy of a dione dianion, precedented for nonbridged diketones, but more likely involves initial dione *O*-silylation followed by bridgehead lithiation-silylation.

(ii) Bridged Lactones, Lactams and Imides. As with the bridgehead enolate chemistry of ketones, we were able to identify a scattering of previous examples of successful bridgehead substitution reactions involving lactone, lactam and imide functions.

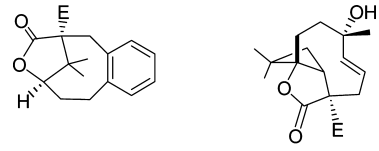

50 **51**

Two relevant examples pertaining to lactones involved substitution of **50** (E = H) using LDA in THF, assisted by HMPA (to give E = methyl, allyl or hydroxyl), and the sulfenylation of hydroxylactam **51** (E = H) to give **51** (E = SPh) as part of a synthesis of the sesquiterpene punctaporonin B.[31,32]

Lactam substitution at bridgehead positions can be found in a number of papers describing synthesis of bridged piperazine-2,5-diones (diketopiperazines, DKPs) of generic structure **52**.

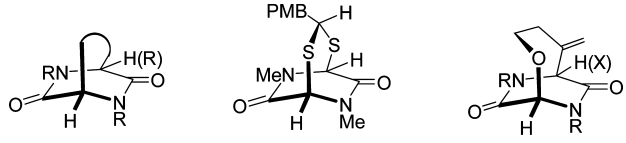

52 **53** **54**

This work originates with metalations of thioacetal bridged DKP **53**, described by Kishi in 1973, en route to a synthesis of gliotoxin.[33] Metalations of [4.2.2] systems of general structure **54** were carried out by the groups of Nakatsuka, Williams, and Hashimoto as a means of accomplishing regio- and stereocontrolled substitution of the bridged DKP core, required for the total synthesis of bicyclomycin.[34−36] Metalation of DKPs with [2.2.2] and [3.2.2] core structures has also been described, attesting to the versatility of these systems.[37,38]

After extensive literature searching we were also able to identify examples of successful lithiation-substitution of bridged imides derived from camphoric acid anhydride, Scheme 11.[39]

Scheme 11

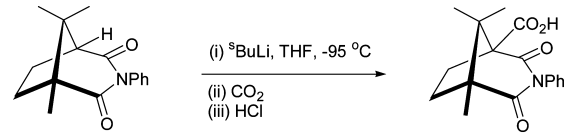

55 **56**

During synthetic studies aimed at the generation of new families of chiral auxiliaries Wanner and Paintner described metalation of the camphanic anhydride-derived imide **55**, using ^{s}BuLi, and subsequent quenching with CO_2. Analogous transformations of the corresponding N−Me and N−H imides, and also a related lactone, were also successful.

With this background we proceeded to examine the metalation chemistry of a range of lactone, lactam and imide derivatives, in a very similar way to the ketone study described earlier. The smallest bridged system selected for study was the 2-azabicyclo[2.2.1]hept-5-en-3-one **57**, having an *N*-phenyl group.[40]

Under various conditions this compound showed no indication of bridgehead metalation, but did undergo very efficient vinylic substitution to give the vinyl silane **58**, Scheme 12. This proved to be the only substitution observed in this lactam family, since extended efforts to effect metalation-silylation of a number of related compounds **59**−**63** proved unsuccessful.

Similar difficulties were experienced with the [2.2.2]-lactam derivatives **64**−**66**, which were readily available from the parent *N*-H lactam.[41] No reaction was observed on treatment of *N*-phenyl derivative **64** with either LDA or LTMP under typical

(29) (a) Rodeschini, V.; Ahmad, N. M.; Simpkins, N. S. *Org. Lett.* **2006**, *8*, 5283. (b) Rodeschini, V.; Simpkins, N. S.; Wilson, C. *J. Org. Chem.* **2007**, *72*, 4265. (c) Ahmad, N. M.; Rodeschini, V.; Simpkins, N. S.; Ward, S. E.; Wilson, C. *Org. Biomol. Chem.* **2007**, *5*, 1924. (d) Ahmad, N. M.; Rodeschini, V.; Simpkins, N. S.; Ward, S. E. *J. Org. Chem.* **2007**, *72*, 4803.
(30) Tsukano, C.; Siegel, D. R.; Danishefsky, S. J. *Angew. Chem., Int. Ed.* **2007**, *46*, 8840.
(31) Khan, F. A.; Czerwonka, R.; Zimmer, R.; Reissig, H.-U. *Synlett* **1997**, 995.
(32) Kende, A. S.; Kaldor, I.; Aslanian, R. *J. Am. Chem. Soc.* **1988**, *110*, 6265.
(33) Kishi, Y.; Fukuyama, T.; Nakatsuka, S. *J. Am. Chem. Soc.* **1973**, *95*, 6490.
(34) Nakatsuka, S.; Yamada, K.; Yoshida, K.; Asano, O.; Murakami, Y.; Goto, T. *Tetrahedron Lett.* **1983**, *24*, 5627.
(35) (a) Williams, R. M.; Armstrong, R. W.; Dung, J.-S. *J. Am. Chem. Soc.* **1985**, *107*, 3253. (b) Williams, R. M.; Dung, J.-S.; Josey, T.; Armstrong, R. W.; Meyers, H. *J. Am. Chem. Soc.* **1983**, *105*, 3214.
(36) Yamaura, M.; Nakayama, T.; Hashimoto, H.; Shin, C.; Yoshimura, J.; Kodama, H. *J. Org. Chem.* **1988**, *53*, 6035.
(37) Eastwood, F. W.; Gunawardana, D.; Wernert, G. T. *Aust. J. Chem.* **1982**, *35*, 2289.
(38) Piccinelli, F.; Porzi, G.; Sandri, M.; Sandri, S. *Tetrahedron:Asymmetry* **2003**, *14*, 393.
(39) (a) Wanner, K. T.; Paintner, F. F. *Tetrahedron* **1994**, *50*, 3113. (b) Wanner, K. T.; Paintner, F. F. *Liebigs Ann.* **1996**, 1941.

Scheme 12

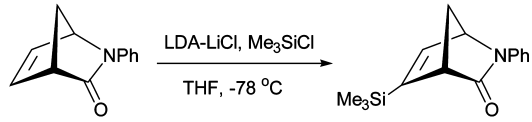

57 **58**

Me_3SiCl in situ quench conditions, whereas *N*-methyl variant **65** showed only low levels of substitution on the methyl group. In the case of the *N*-benzyl compound this type of reactivity was much more pronounced, and clean conversion of **66** into the silylated product **67** was observed, Scheme 13.

Scheme 13

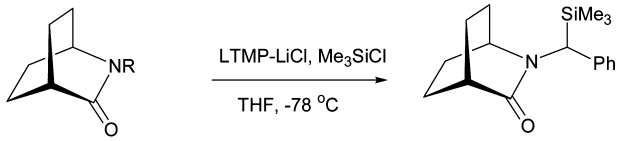

64 R = Ph
65 R = Me
66 R = Bn

67

More success was seen with the [3.2.1] and [3.3.1] systems **68**−**71**, which were readily prepared in the form of *N*-phenyl lactams **68** and **69**, or lactones **70** and **71**. In each case, the starting material (E = H) was converted into the bridgehead silylated product (E = $SiMe_3$) by the action of either LDA or LTMP.

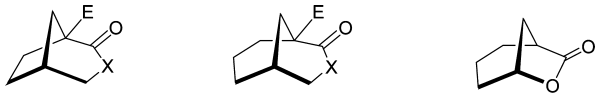

68 X = NPh (87%)
70 X = O (32%)

69 X = NPh (74%)
71 X = O (61%)

72

The *N*-phenyl lactams proved particularly good substrates for this chemistry, presumably due to a combination of metalation viability and robustness of the lithiated intermediates toward side-reactions such as self-condensation. The corresponding lactones gave lower yields, and some evidence of side reactions (presumably involving ring-opening) was evident. The lactone **72** in which the carbonyl function is constrained in the smallest (two atom) bridge gave no substitution product, and was completely destroyed in the metalations attempted.

Finally, we moved on to spend considerable time exploring the bridgehead substitution chemistry of bridged imides. To some extent, our earlier exploration of the chemistry of the cyclopropane fused imide **73** had acted as an additional prompt in the direction of nonplanar enolate chemistry, this system behaving well in substitution reactions—including those mediated by chiral bases, Scheme 14.[24]

Scheme 14

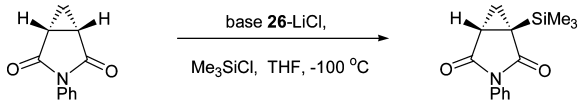

73

74, 80%, 91-95% ee

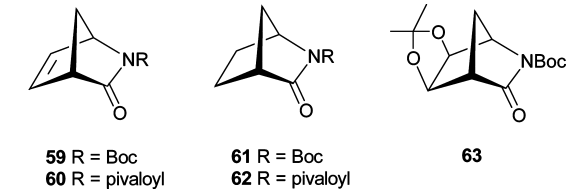

59 R = Boc
60 R = pivaloyl

61 R = Boc
62 R = pivaloyl

63

Table 2

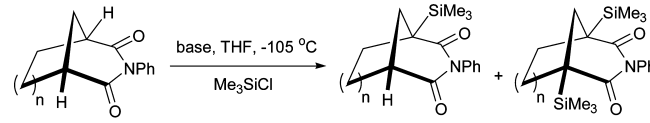

75 n = 1
76 n = 2

77 n = 1
78 n = 2

79 n = 1
80 n = 2

entry	imide	base	**77/78** (%)	ee (%)	**79/80** (%)
1	**75**	LTMP	rac-**77** (16)	−	**79** (20)
2	**75**	(*R*,*R*)-**26**	(−)-**77** (63)	70	**79** (18)
3	**75**	**39**	(+)-**77** (47)	94	**79** (24)
4	**76**	LTMP	rac-**78** (47)	−	**80** (20)
5	**76**	(*R*,*R*)-**26**	(−)-**78** (74)	98	**80** (12)
6	**76**	(*S*,*S*)-**26**	(+)-**78** (56)	98	**80** (15)

This reaction gives good yields and selectivities in the generation of silyl-substituted imide **74**, despite the fact that an in situ quench is required to stop the intermediate anion undergoing self-destruction (presumably by uncontrolled condensation processes).

We began analogous studies of the bridged imide counterparts by examining the silylation of imides **75** and **76**, having [3.2.1] and [3.3.1] structures respectively, Table 2.

For both starting imides the yields of monosilylated imides that could be achieved using LTMP were modest, especially for the smaller imide **75**. In this case we also tried using ^{s}BuLi as base, as utilized in the camphanic imide studies highlighted in Scheme 11, but we observed imide ring-opening in place of silylation.

Fortunately, our chiral lithium amides gave rather better yields of products **77** or **78**, although always accompanied by lesser quantities of doubly silylated imides **79** or **80**. The simple chiral base **26** gave a reasonable ee with the smaller imide, but gave excellent results with the [3.3.1]-imide, either enantiomer being available in >98% ee. For the smaller system we also showed that swapping to the *bis*-lithium amide **39** gave (+)-**77** in an excellent 94% ee.

In all cases, the precise outcome of the reaction was somewhat variable, depending upon temperature, time of addition, etc. Maintaining a very low temperature by means of liquid nitrogen slush baths appears important for optimal results; a repeat of entry 5 at −78 °C gave the product in reduced yield (53%) and a slightly reduced ee (90%). In the case of chiral base reactions, we cannot rule out a small degree of kinetic resolution being superimposed on the initial enantiotopic hydrogen discriminating event.[42]

Both the bridgehead silanes (−)-**77** and (−)-**78** obtained using base (*R*,*R*)-**26** provided crystalline samples suitable for X-ray analysis. The structures of these compounds, including absolute stereochemistry, are shown in Figure 5.

Despite the obvious stereoelectronic differences between these bridgehead metalations and more conventional imide (or ketone) deprotonations, the sense of stereoinduction observed displays

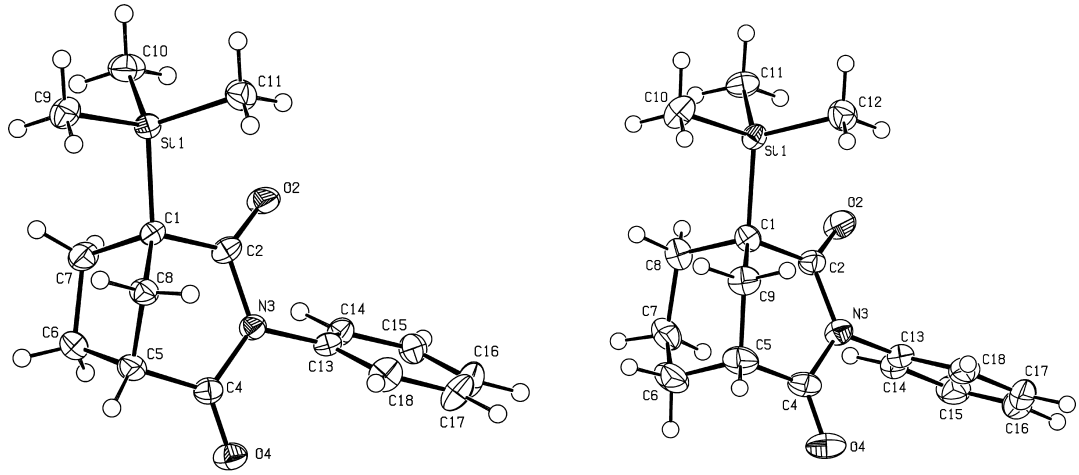

Figure 5. X-ray structure of (−)-**77** and (−)-**78**.

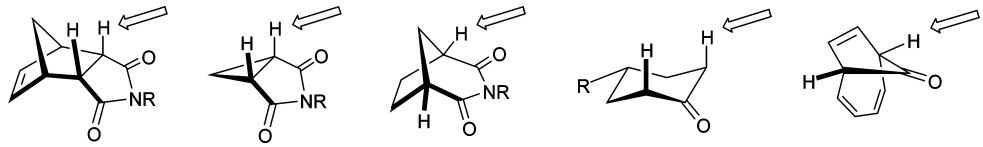

Figure 6. Sense of proton removal in reactions of base (*R*,*R*)-**26** with various substrates.

Table 3

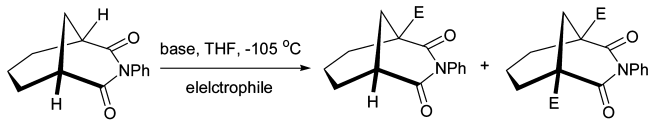

76 **81-85** **86-90**

entry	base	electrophile	**81**−**85** (%)	ee (%)	**86**−**90** (%)
1	LTMP	MeI	**81** (40)	−	**86** (25)
2	(*R*,*R*)-**26**	MeI	**81** (57)	97	**86** (11)
3	LTMP	allyl bromide	**82** (25)	−	**87** (13)
4	(*R*,*R*)-**26**	allyl bromide	**82** (42)	95	**87** (7)
5	LTMP	prenyl bromide	**83** (42)	−	**88** (19)
6	(*R*,*R*)-**26**	prenyl bromide	**83** (50)	98	**88** (12)
7	LTMP	BnBr	**84** (54)	−	**89** (19)
8	(*R*,*R*)-**26**	BnBr	**84** (52)	95	**89** (3)
9	LTMP	pivaloyl chloride	**85** (23)	−	**90** (34)
10	(*R*,*R*)-**26**	pivaloyl chloride	**85** (56)	98	**90** (17)

clear parallels with the results from previous studies. For ease of comparison, selected results are reiterated in Figure 6.

In all of the imide chemistry described so far, we had concentrated on the use of silicon as an in situ electrophile. Although we were interested in the use of alternative electrophiles, neither **75** or **76** showed product formation under conventional external quench conditions, using a number of alkylating or acylating agents. We subsequently established that for imide **76** it was possible to extend the in situ quench protocol to a narrow range of additional electrophiles, Table 3.

Yields were moderate, with the chiral base usually giving better results than LTMP, but the levels of asymmetric induction were quite uniform and always at least 95% ee. We were unable to achieve analogous substitution chemistry with the smaller, more rigid, [3.2.1]-imide starting material **75**.

The reasons behind the success of this improvised in situ quench method, compared to the recovery of starting imide when conventional external quenching is employed (i.e., the use of a distinct metalation period before addition of the electrophile) is unclear. One possibility is that the metalation involves an unfavorable equilibrium (due to the borderline anion stabilization available), which is only 'pulled' in the direction of product if electrophile is available (and to some extent compatible with the lithium amide).

These results, combined with the possibility of using the fluoride-mediated silyl substitution method (e.g., Table 1), convinced us that bridgehead substitution with carbon electrophiles should be possible in many cases, and was an important factor in our plans for the total synthesis of clusianone and welwistatin, mentioned earlier.

A few additional examples of both approaches to nonsilicon bridgehead substituents are shown in Scheme 15.

For imide **78** we were able to demonstrate additional substitution to generate **91** and **92**. These reactions proceeded in noticeably higher yields than those detailed in Table 3, there being no possibility of over-reaction to give doubly alkylated products. Substitution of the silicon substituent in **77** and **78** was possible by use of a CsF method that we had employed previously with silylcyclopropanes like **74**, the use of either TBAF or TBAT resulting only in proto-desilylation in these cases.

In our previous work on chiral silylated imides we had observed that the silicon substituent exerts complete control of the regiochemistry of imide addition chemistry-for example involving DIBAL-H reduction or reaction with Grignard reagents.[24,42] We were pleased to find that the same type of control was also evident in the reactions of the silylated bridged imides (−)-**77** and (−)-**78**, Scheme 16.

Reduction of **77** or **78** proved high yielding and gave only the regioisomer of **95** or **96** expected (as a mixture of epimers), further reduction then gave the lactams **68** or **69** mentioned earlier but this time in optically active form. HPLC analysis

Scheme 15

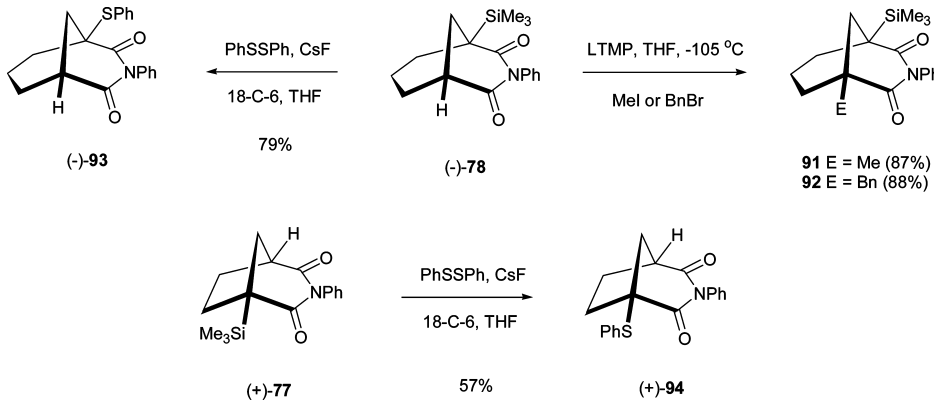

Scheme 16

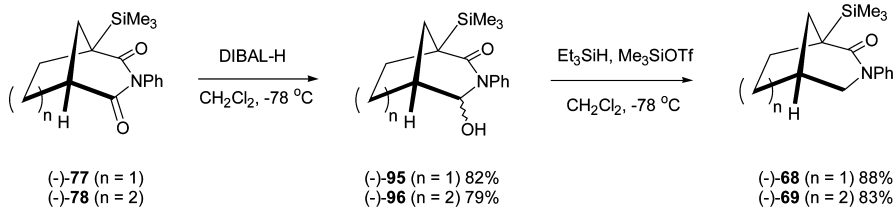

confirmed that the levels of enantiomeric enrichment seen in the imides **77** and **78** was translated into the lactam products **68** and **69** with complete fidelity.

Finally, we also showed that reaction of **77** or **78** with Lawesson's reagent in toluene at reflux led to the production of the monothioimides **97** and **98** respectively, the sense of regioselectivity being confirmed for **98** by an X-ray structure determination, Figure 7.[43]

An interesting feature of the ^{1}H NMR spectrum of **98** was the appearance of the *ortho* hydrogens of the *N*-phenyl group appearing as rather broad nonequivalent signals at δ 6.96 and 7.18. This is presumably due to atropisomerism about the aryl N−C bond, caused by the introduction of the sulfur atom.

This completed the survey of bridgehead substitution reactions possible to us with the resource available. Despite the failure of some systems to metalate, *the overall picture revealed by the silylations described above is that a remarkable range of varied bridged carbonyl compounds will undergo unexpected (from a classical point of view) bridgehead metalation-substitution*.

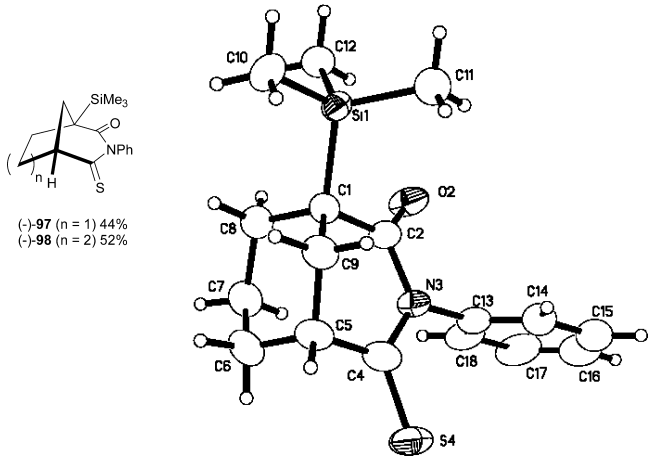

Figure 7. X-ray structure of (−)-**98**.

Computational Insight into Bridgehead Deprotonation

Having carried out a substantial survey of bridgehead metalations of various types of carbonyl compound we identified some trends and some slightly puzzling aspects. Clearly, metalation of systems with small bridges ($S = 5$) is not synthetically useful, with camphenilone seemingly a borderline viable case, and the [2.2.1] lactams **57** and **59**−**63** all giving negative results. Although we did not make the [2.2.1] lactone, the failure of the [3.2.1] higher homologue **72**, and the apparent susceptibility of this compound to ring-opening surely predicates against success with the smaller lactone. The contrast between the [3.2.1] lactone **72** with the carbonyl function in the two atom bridge, compared to the successful silylation of the isomer **70** with the lactone in the three atom bridge, appears to argue for flexibility around the carbonyl function as one important criterion for metalation - perhaps crucial for some degree of rehybridization in the 'enolate'. The failure of ketone and lactam [2.2.2] systems, **14** and **64**−**66**, seems to fit with this idea, in both cases the carbonyl is constrained in a two atom bridge. If the ketone carbonyl is the sole bridging atom, as in [3.3.1] ketone **15**, we would therefore expect metalation to be problematic- and this was the case with this system. However, more extended systems, such as **37** or **42** gave good results, and even a modified [3.3.1] system **46**, which might be regarded as doubly activated, behaved well in substitution chemistry. It seems apparent that compounds where the activating carbonyl is in at least a three atom bridge can be relied upon to react, and compounds where S is at least 7 appear mainly viable.

However, more in-depth consideration of the results seemed to reveal unsatisfactory aspects of our superficial analysis For example, if some level of flexibility in the carbonyl-containing bridge was required, then why were the (seemingly rigid) bicyclic imides such good substrates? If we accept the *S* value as a guide to metalation then why should a [3.2.1] lactam be more competent than a [2.2.2] relative?

To try and address the fundamental reasons for this reactivity, and to try and explain some of the puzzling aspects outlined above,

Scheme 17. Hypothetical Deprotonation Reaction of Bridgehead Carbonyl **99** with Dimethyl Amide **100**

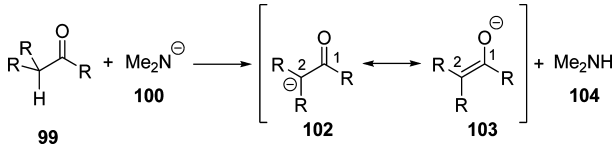

we conducted a compuational analysis (B3LYP) of the brigehead deprotonation reactions.

Computational Methods. Geometry optimizations were performed using either B3LYP/6-31G* or B3LYP/6-31+G* level of theory using Spartan '04 (Windows),[44] and single point B3LYP/6-31+G* energies were also calculated for a range of the B3LYP/6-31G* optimized structures. Zero point vibrational energies were calculated for all structures and the absence of imaginary frequencies was used to characterize the structures as minima on their potential energy surfaces. NBO[45] calculations were performed on all anionic species using the NBO keyword in Spartan '04 (Windows).

Modeling of Bridgehead Deprotonations. B3LYP calculations have enabled us to start to rationalize our bridgehead metalation results by calculating the ΔE_{rxn} value (kcal mol^{-1}) for the simplified deprotonation reaction shown in Scheme 17.

For the sake of computational expediency we made a number of simplifications compared to the systems employed experimentally, namely the use of N−Me rather than N−Ph for the lactams and imides and the use of a simpler amide base (dimethyl amide). More significantly, anions were treated as metal (and solvent) free, monomeric species, and while this may seem a substantial departure from reality, these types of simplification have been employed previously to good effect in the organometallic field by von R. Schleyer, who showed that the calculated energies of simple organolithiums and those of the corresponding carbanions parallel each other closely.[46a] Although we are mindful that there are likely to be significant differences between the structures of the free anionic and corresponding lithiated species,[46b] the close match between the experimentally observed results and those obtained by our calculations seem to validate our computational approach (*vide infra*).

Our first task was to decide upon an appropriate level of theory to use in our study, and we began by comparing the results of B3LYP/6-31+G*//B3LYP/6-31+G*, B3LYP/6-31+G*//B3LYP/6-31G* and B3LYP/6-31G*//B3LYP/6-31G* calculations on an initial selection of deprotonations (Table 4). It became immediately apparent that ΔE_{rxn} values calculated using B3LYP/6-31+G*//B3LYP/6-31G* showed very good agreement with those obtained for the fully optimized B3LYP/6-31+G*//B3LYP/6-31+G* structures (gradient = 1.0006, $R^2 = 1$, Figure 8a, Table 4). Furthermore, the values of ΔE_{rxn} calculated using B3LYP/6-31G*//B3LYP/6-31G* also correlated well with those calculated with the larger basis set (gradient = 1.0456, $R^2 = 0.997$, Figure 8b, Table 4), with ΔE_{rxn} being systematically underestimated by 2.28 kcal mol^{-1}.

Table 4. Comparison of ΔE_{rxn} Calculated at B3LYP/6-31+G*//B3LYP/6-31+G*, B3LYP/6-31+G*//B3LYP/6-31G* and B3LYP/6-31G*//B3LYP/6-31G*

		6-31+G*//6-31+G*	6-31+G*//6-31G*	6-31G*//6-31G*	
entry	carbonyl	ΔE_{rxn} (kcal mol^{-1})	ΔE_{rxn} (kcal mol^{-1})	ΔE_{rxn} (kcal mol^{-1})	Δzpe_{rxn} (kcal mol^{-1})
1	**1**	2.74	2.62	0.98	1.18
4	**15**	7.43	7.28	4.65	2.10
6	**20**	−9.20	−9.31	−12.31	1.53
7	**61**	5.59	5.50	4.16	1.07
8	**70**	−7.98	−8.15	−10.4	1.45
9	**71**	−14.1	−14.2	−17.1	1.50
10	**75**	−13.2	−13.3	−16.0	1.86

Satisfied by these initial results, we chose to use B3LYP/6-31G*//B3LYP/6-31G* for all subsequent calculations as it was computationally efficient, and we were safe in the knowledge that if required we could obtain the corresponding 6-31+G* ΔE_{rxn} by performing relatively inexpensive 6-31+G* single point calculations or we could obtain a good estimate by simply adding 2.28 kcal mol^{-1} to the 6-31G* ΔE_{rxn} value.

Having defined our computational approach, we then calculated ΔE_{rxn} values for a wider range of ketone (Table 5), lactam (Table 6), lactone (Table 7) and imide (Table 8) bridgehead deprotonations. In order to access key reference data (ΔE_{rxn} values, bond length changes etc.) calculations were also performed on the deprotonation reactions of cyclohexanone **105**, *N*-methyl-δ-valerolactam **106**, δ-valerolactone **107** and *N*-methyl-glutarimide **108** (Figure 9).

It can be seen from these calculated data that a wide range of ΔE_{rxn} values are obtained, with some examples having large negative values and some having substantial positive values. Furthermore, there is a very good correlation between the theoretical viability of a given deprotonation reaction (−ve ΔE_{rxn} = favorable; +ve ΔE_{rxn} = unfavorable) and the actual experimental outcome observed. For example, calculations on ketones **16**, **17**, **20**, **21** and **42** all give negative ΔE_{rxn} values and all undergo effective bridgehead metalation and substitution, whereas ketones **13**, **14** and **15**, which have positive ΔE_{rxn} values, do not. Camphenilone **1** (ΔE_{rxn} = + 0.98 kcal mol^{-1}) has a small positive value, indicative of a borderline situation, and this is in line with the observation that this compound metallates, but self-condenses uncontrollably. The ability to account for the sharp difference in reactivity seen in the laboratory between the isomeric [3.3.1] **15** (+4.65 kcal mol^{-1}) and [4.2.1] **20** (−12.31 kcal mol^{-1}) ketones (both having $S = 7$ according to the Bredt classification) is particularly satisfying and bodes well for the future predictive value of this computational approach. Similarly good results are obtained with the lactams, lactones and imides (Tables 6−8), with close parallels being observed between the calculated and experimental behavior of the carbonyls being studied. For example, the inability to metalate the [2.2.1] **59**, **61** and the [2.2.2] **65** lactams is supported by the positive calculated ΔE_{rxn} values (Table 6), while the negative ΔE_{rxn} values obtained for all other lactams (Table 6), lactones (Table 7) and imides (Table 8) correlate well with their successful deprotonations in the laboratory.

In addition to simply predicting whether deprotonation reactions are favorable or not, the B3LYP calculations also provide structural information on the anions produced, and this data would be quite difficult to obtain experimentally. Our analysis of the calculated structures began with a simple survey of the C^1-C^2 bond lengths in the deprotonated species, which could be visualized as the resonance hybrid of the α-keto anion **102** and the enolate **103** (Scheme 17). The shortest C^1-C^2 bond length calculated was that derived from *N*-methyl-glutarimide **108** (1.38 Å) and the longest was that derived from the unsaturated [2.2.1] lactam **59** (1.51 Å). A plot of ΔE_{rxn} versus C^1-C^2 bond length (Figure 10a) shows that, in general, deprotonations are favorable when the C^1-C^2 bond length is shorter than 1.45 Å. It is probably

(40) Chan, D. M. T.; Monaco, K. L.; Wang, R.-P.; Winters, M. P. *Tetrahedron Lett.* **1998**, *39*, 2933.
(41) Werner, L. H.; Ricca, S., Jr. *J. Am. Chem. Soc.* **1958**, *80*, 2733.
(42) Gill, C. D.; Greenhalgh, D. A.; Simpkins, N. S. *Tetrahedron* **2003**, *59*, 9213.
(43) Milewska, M. J.; Gdaniec, M.; Polonski, T. *J. Org. Chem.* **1997**, *62*, 1860.
(44) *Spartan '04*; Wave Function, Inc.: Irvine, CA, 2004. Kong, J.; et al. *J. Comput. Chem.* **2000**, *21*, 1532.
(45) (a) Foster, J. P.; Weinhold, F. *J. Am. Chem. Soc.* **1980**, *102*, 7211. (b) Reed, A. E.; Weinstock, R. B.; Weinhold, F. *J. Chem. Phys.* **1985**, *83*, 735. (c) Reed, A. E.; Curtiss, L. A.; Weinhold, F. *Chem. Rev.* **1988**, *88*, 899. (d) Weinhold, F.; Landis, C. R. *Chem. Ed.: Res. Pract.* **2001**, *2*, 91.
(46) (a) Schleyer, P. v. R.; Chandrasekhar, J.; Kos, A. J.; Clark, T.; Spitznagel, G. W. *J. Chem. Soc., Chem. Commun.* **1981**, 882. (b) Lambert, C.; Schleyer, P. v. R. *Angew. Chem., Int. Ed.* **1994**, *33*, 1129.

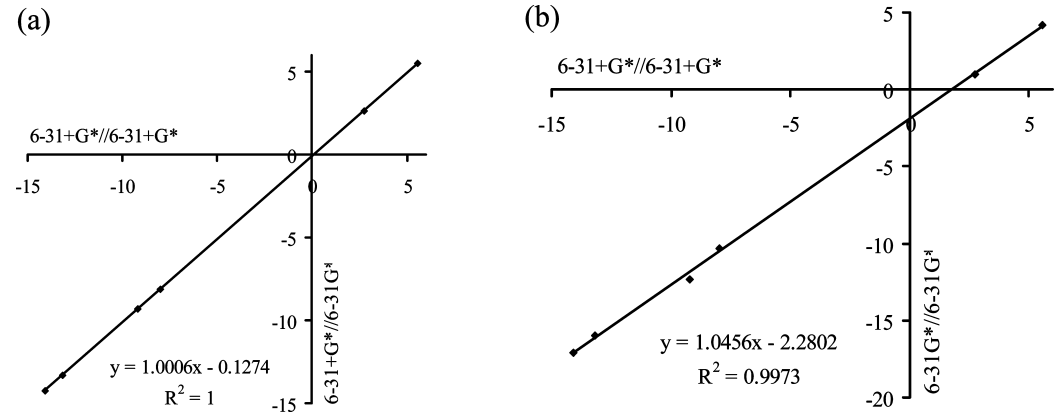

Figure 8. Comparisons of ΔE_{rxn} (kcal mol^{-1}) at (a) B3LYP/6-31+G*//B3LYP/6-31+G* and B3LYP/6-31+G*//B3LYP/6-31G*; (b) B3LYP/6-31+G*//B3LYP/6-31+G* and B3LYP/6-31G*//B3LYP/6-31G*.

Table 5. B3LYP/6-31G*//B3LYP/6-31G* Calculated ΔE_{rxn} Values and Key Bond Length Data for Ketone Deprotonation

entry	carbonyl	ΔE_{rxn} (kcal mol^{-1})	Δzpe_{rxn} (kcal mol^{-1})	C−C (Å)	ΔC−C (Å)	% shortening	C−O (Å)	ΔC−O (Å)	% lengthening
1	**1**	0.976	1.18	1.47	0.061	4.0	1.24	0.027	2.2
2	**13**	2.33	1.36	1.45	0.068	4.5	1.25	0.031	2.6
3	**14**	7.83	1.18	1.46	0.061	4.0	1.25	0.028	2.3
4	**15**	4.65	2.10	1.44	0.078	5.1	1.25	0.036	3.0
5	**17**	−12.3	1.58	1.42	0.118	7.7	1.27	0.047	3.9
6	**16**	−10.2	1.63	1.42	0.102	6.7	1.26	0.043	3.5
7	**20**	−12.3	1.53	1.42	0.115	7.5	1.26	0.045	3.7
8	**21**	−19.0	1.36	1.46	0.075	4.9	1.23	0.025	2.1
9	**42**	−12.4	1.27	1.41	0.124	8.1	1.26	0.047	3.9
10	**105**	−27.5	2.08	1.39	0.136	8.9	1.27	0.055	4.5

Table 6. B3LYP/6-31G*//B3LYP/6-31G* Calculated ΔE_{rxn} Values and Key Bond Length Data for Lactam Deprotonation

entry	carbonyl	ΔE_{rxn} (kcal mol^{-1})	Δzpe_{rxn} (kcal mol^{-1})	C−C (Å)	ΔC−C (Å)	% shortening	C−O (Å)	ΔC−O (Å)	% lengthening
1	**59**	1.00	1.38	1.51	0.041	2.6	1.23	0.014	1.2
2	**61**	4.16	1.07	1.49	0.044	2.9	1.24	0.016	1.3
3	**65**	8.37	0.945	1.49	0.042	2.8	1.24	0.015	1.2
4	**68**	−2.57	1.11	1.43	0.097	6.3	1.25	0.025	2.0
5	**69**	−8.95	1.23	1.41	0.119	7.8	1.26	0.031	2.5
6	**106**	−19.5	1.51	1.39	0.14	9.2	1.26	0.037	3.0

Table 7. B3LYP/6-31G*//B3LYP/6-31G* Calculated ΔE_{rxn} Values and Key Bond Length Data for Lactone Deprotonation

entry	carbonyl	ΔE_{rxn} (kcal mol^{-1})	Δzpe_{rxn} (kcal mol^{-1})	C−C (Å)	ΔC−C (Å)	% shortening	C−O (Å)	ΔC−O (Å)	% lengthening
1	**70**	−10.3	1.45	1.42	0.101	6.6	1.23	0.026	2.2
2	**71**	−17.1	1.50	1.40	0.122	8.0	1.24	0.032	2.6
3	**72**	−6.66	1.16	1.45	0.085	5.5	1.23	0.022	1.8
4	**107**	−29.0	1.95	1.39	0.139	9.1	1.24	0.037	3.1

Table 8. B3LYP/6-31G*//B3LYP/6-31G* Calculated ΔE_{rxn} Values and Key Bond Length Data for Imide Deprotonation

entry	carbonyl	ΔE_{rxn} (kcal mol^{-1})	Δzpe_{rxn} (kcal mol^{-1})	C−C (Å)	ΔC−C (Å)	% shortening	C−O (Å)	ΔC−O (Å)	% lengthening
1	**73**	−22.5	2.19	1.46	0.042	2.8	1.23	0.023	1.9
2	**75**	−16.0	1.86	1.42	0.099	6.5	1.24	0.025	2.1
3	**76**	−22.9	1.73	1.40	0.125	8.2	1.25	0.031	2.5
4	**108**	−37.4	2.02	1.38	0.143	9.4	1.26	0.038	3.1

more meaningful, however, to look at the relative bond length change upon deprotonation as this explicitly takes into account structural variations in both the starting carbonyl and the anionic product. Figure 10b shows how ΔE_{rxn} varies as a function of the percentage shortening of the C^1-C^2 bond, and it can be seen that the maximum shortening is 9.4% for *N*-methyl-glutarimide **108** and the minimum shortening is 2.6% for the unsaturated lactam **59**. Generally speaking, favorable deprotonations are usually accompanied by shortenings of greater than 5%, while unfavorable deprotonations show shortenings of less than 5% relative to the original carbonyl.

Deprotonation of the [3.1.0] imide **73**, however, provides one notable exception to this general trend. The calculated ΔE_{rxn} (−22.5 kcal mol^{-1}) indicates a very favorable deprotonation, and indeed

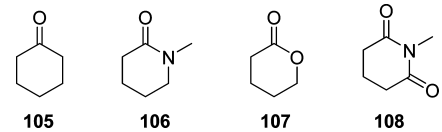

Figure 9. Structures of reference carbonyl compounds used in calculations.

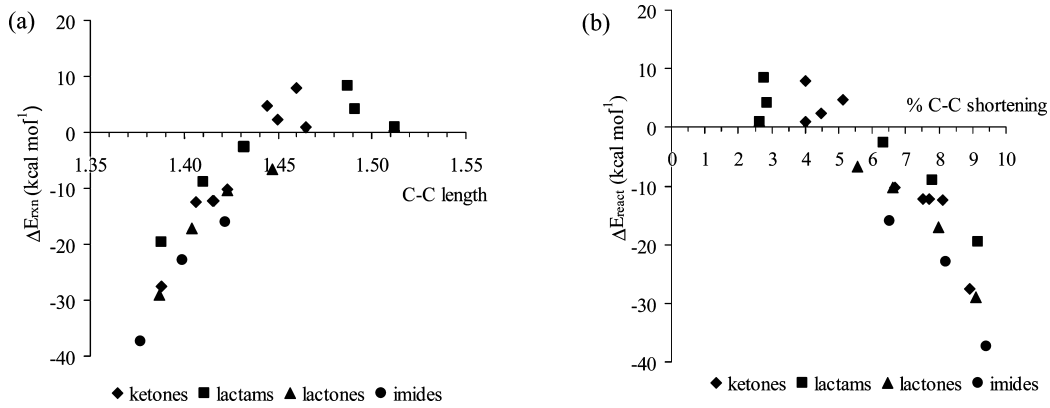

Figure 10. (a) Plot of ΔE_{rxn} (kcal mol^{-1}) versus C^1−C^2 bond length (Å); (b) plot of ΔE_{rxn} (kcal mol^{-1}) versus % shortening in C^1−C^2 bond length upon deprotonation.

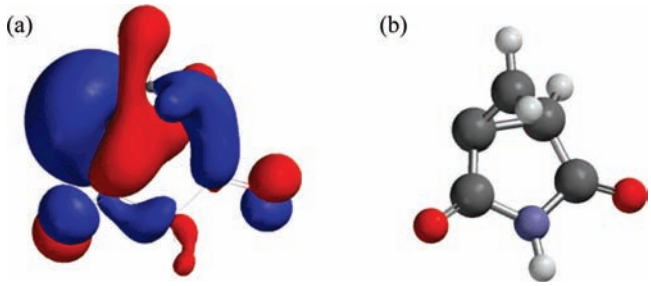

Figure 11. (a) Representation of the HOMO calculated for [3.1.0] imide anion **109** (B3LYP/6-31G*). (b) Ball and spoke representation of [3.1.0] imide anion **109** (B3LYP/6-31G*).

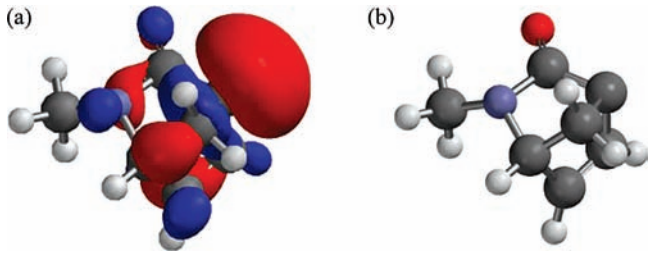

Figure 12. (a) Representation of HOMO calculated for [2.2.1] lactam anion **113** (B3LYP/6-31G*). (b) Ball and spoke representation of [2.2.1] lactam anion **113** (B3LYP/6-31G*).

this is confirmed by the successful deprotonation-silylation experiment performed previously (Scheme 14). Calculations suggest a C^1−C^2 bond length shortening of only 2.8% upon conversion to the anionic species **109** (Scheme 2), and according to the trend suggested by Figure 10 (b), this should equate to an unfavorable situation in terms of ΔE_{rxn}.

A closer analysis of the calculated structure of **109** reveals the fact that in addition to the proximal imide carbonyl, both the cyclopropane ring and the distal imide carbonyl are involved in delocalizing, and hence stabilizing, the negative charge. These effects manifest themselves in corresponding bond shortenings and bond lengthenings. For example, C^1−C^2, C^2−C^5 and C^3−C^4 shorten by 2.8%, 0.9% and 1.4% respectively, while C^2−C^3 and C^3−C^5 lengthen by 1.3% and 1.58% respectively. A representation of the HOMO of **109** is shown in Figure 11a and the involvement of the cyclopropane and both carbonyls can clearly be seen in this molecular orbital.

A simplified way of visualizing this stabilization can be obtained by considering the resonance structures (**109**−**112**) in Scheme 18. Prompted by the somewhat obvious realization that a number of structural factors (other than enolate formation) can stabilize carbanions, we re-examined our data and found that, while the

Scheme 18

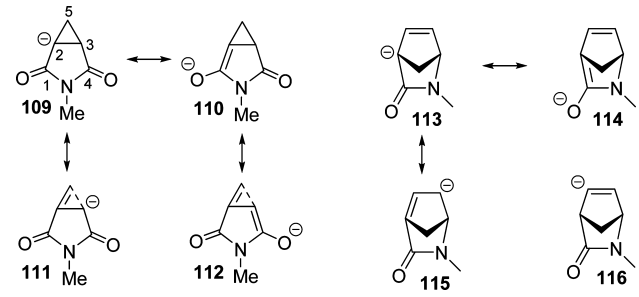

Table 9. Calculated ΔE_{rxn} (kcal mol^{-1}) and NBO Analysis for Bridged Ketones

entry	carbonyl	ΔE_{rxn} (kcal mol^{-1})	Δzpe_{rxn} (kcal mol^{-1})	C=C occupancy	carbanion occupancy
1	**1**	0.976	1.18	−	1.672
2	**13**	2.33	1.36	−	1.658
3	**14**	7.83	1.18	−	1.775
4	**15**	4.65	2.10	−	1.757
5	**17**	−12.25	1.58	−	1.458
6	**20**	−12.3	1.53	−	1.444
7	**21**	−19.0	1.36	−	1.387
8	**16**	−10.2	1.63	−	1.481
9	**42**	−12.4	1.27	1.872	−
10	**105**	−27.5	2.08	1.927	−

Table 10. Calculated ΔE_{rxn} (kcal mol^{-1}) and NBO Analysis for Bridged Lactams, Lactones and Imides

entry	carbonyl	ΔE_{rxn} (kcal mol^{-1})	Δzpe_{rxn} (kcal mol^{-1})	C=C occupancy	carbanion occupancy
1	**61**	4.16	1.07	−	1.7654
2	**64**	8.37	0.945	−	1.735
3	**68**	−2.57	1.11	1.863	−
4	**69**	−8.95	1.23	1.889	−
5	**106**	−19.5	1.51	1.938	−
6	**70**	−10.4	1.45	1.877	−
7	**71**	−17.1	1.50	1.898	−
8	**72**	−6.7	1.16	−	1.643
9	**107**	−29.0	1.95	1.943	−
10	**75**	−16.0	1.86	1.865	−
11	**76**	−22.9	1.73	1.899	−
12	**108**	−37.4	2.02	1.943	−

ΔE_{rxn} (+1.0 kcal mol^{-1}) suggested an unfavorable deprotonation for the unsaturated lactam **59**, it did however appear to be more favorable than its change in C^1−C^2 bond length ($\Delta_{C^1-C^2}$ = 0.041 Å, 2.6% shortening) would suggest.

The source of the added stabilization is more obvious in this case, as it appears that the anion can be partially delocalized around

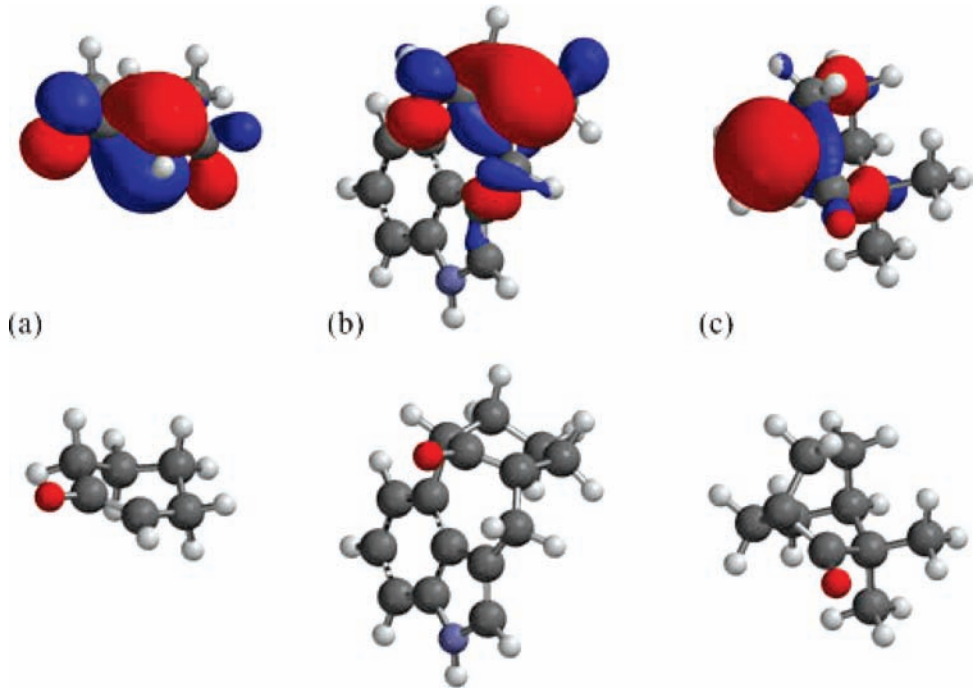

Figure 13. (a) HOMO and ball and spoke representations of deprotonated cyclohexanone **105**. (b) HOMO and ball and spoke representations of deprotonated ketone **42**. (c) HOMO and ball and spoke representations of deprotonated [2.2.2] ketone **14**. All calculated at B3LYP/6-31G*.

the embedded allylic system (Figure 12). Further analysis of this particular example was considered unnecessary as the ΔE_{rxn} (−6.8 kcal mol^{-1}) calculated for deprotonation of the vinylic group in **59** to give anion **116** (Scheme 18) clearly indicated that bridgehead metalation of **59** was unlikely to be synthetically useful, and this was confirmed in the laboratory by the formation of **58** (Scheme 12).

In addition to correlating ΔE_{rxn} to bond length changes upon deprotonation, we also performed natural bond orbital (NBO)[45] analysis on the calculated anion structures to gain a further level of insight into the nature of the anionic species (Tables 9 and 10). The results of NBO analysis for the ketone series are presented in Table 9, and they clearly show that the majority of deprotonated species are best represented as the α-keto carbanionic form **102** rather than the more familiar enolate form **103** (Scheme 17). Only the anion derived from ketone **42** and that derived from cyclohexanone **105** are best represented as enolate structures, based upon occupancy of the C═C of the enolate double bond (1.872 and 1.927 electrons respectively).

The differences highlighted by the NBO calculations can also be seen in the HOMOs of the various anionic species. For example, the HOMO of deprotonated cyclohexanone (Figure 13a) corresponds to the familiar description expected for an enolate. It is clearly dominated by the π-type overlap of two $2p_z$ orbitals, one from each of the two carbon atoms, and one $2p_z$ orbital from the oxygen atom that makes up the enolate.

A very similar looking HOMO is obtained for deprotonated **42** (Figure 13b) and the π-bond corresponding to C^1-C^2 (Scheme 1) of the enolate can be clearly seen. In contrast to this, the HOMO of the deprotonated [2.2.2] ketone **14** (Figure 13c) shows a clear lack of π-bonding character between C^1 and C^2, and appears to correspond to an anion accommodated in an orbital system that is orthogonal to the π-bonding framework of the carbonyl. These examples represent extremes within the ketone series, and representations of the HOMOs of other members lie somewhere between the two.

One added bonus of the NBO analysis is that it not only provides a qualitative description of the structure of the anionic species, but it also gives valuable quantitative data that can be used to predict the order of anion stability. A plot of ΔE_{rxn} versus C^2 carbanion electron occupancy (Table 9, Figure 14) gives a

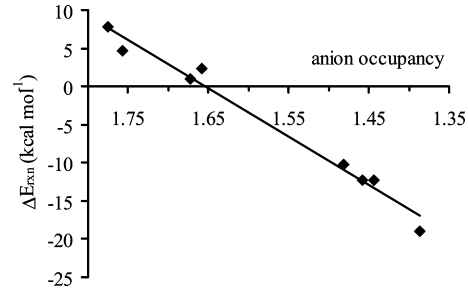

Figure 14. Plot of ΔE_{rxn} (kcal mol^{-1}) versus anion electron occupancy (NBO calculations, B3LYP/6-31G*) at C^2 of deprotonated ketones (R^2 = 0.9796).

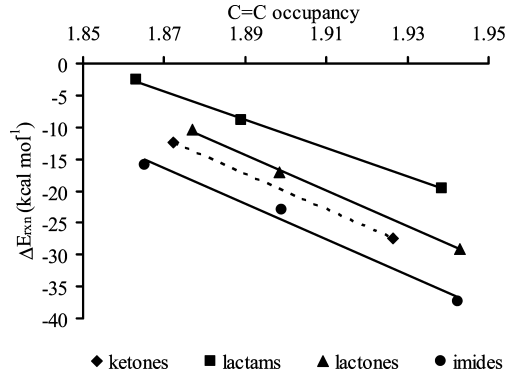

Figure 15. Plots of ΔE_{rxn} (kcal mol^{-1}) versus C═C electron occupancy (NBO calculations, B3LYP/6-31G*) of deprotonated ketones, lactams (R^2 = 0.9988), lactones (R^2 = 0.9982) and imides (R^2 = 0.9836).

linear correlation (R^2 = 0.9796) over the range observed, and this can be then used to predict ΔE_{rxn} if the ketone anion occupancy is known from NBO calculations.

This could provide a very useful predictive tool for experimentalists, as only a single B3LYP/6-31G* calculation is required in order to determine the carbanion electron occupancy via NBO analysis, and this can then be used in conjunction with

Scheme 19. Williams's Deprotonation of Diketopiperazines **117** and **118** and Anion Equilibration

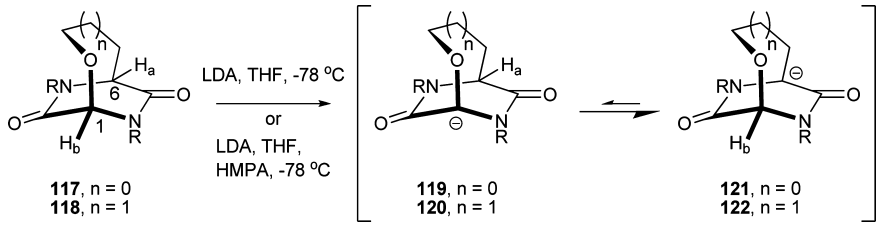

Table 11. Calculated ΔE_{rxn} (kcal mol^{-1}) and NBO Analysis for Williams's Bridged Diketopiperazines

entry	carbonyl	anion	ΔE_{rxn} (kcal mol^{-1})	Δzpe_{rxn} (kcal mol^{-1})	C=C occupancy	carbanion occupancy
1	**117**	**119**	−16.1	1.55	−	1.670
2	**117**	**121**	−20.7	1.52	−	1.689
3	**118**	**120**	−24.3	1.97	1.905	−
4	**118**	**122**	−31.0	1.79	1.885	−

Figure 14 to provide an estimate for ΔE_{rxn}. The calculated C^1-C^2 (Scheme 1) bond length can also be used in conjunction with Figure 10a to provide a double check for the viability of a proposed deprotonation reaction. As the remaining ketones, and the majority of lactams, lactones and imides are judged to be best represented as enolates by NBO analysis, we constructed similar plots of ΔE_{rxn} versus C=C electron occupancy of the putative enolate-like structures (Table 10, Figure 15).

As for the ketone-derived carbanion series (Figure 14), there appears to be a linear correlation between ΔE_{rxn} and the C=C occupancy of the lactam ($R^2 = 0.9988$), lactone ($R^2 = 0.9982$) and imide ($R^2 = 0.9836$) series of compounds. The two data points for the deprotonated ketones **42** and cyclohexanone **105** (Table 9) have also been plotted in Figure 15 and the dotted line simply connects the two points. Although there is not enough data to justify attaching any significance to this line, it is striking that it is very close to being parallel to those lines derived from the other carbonyl species. As suggested before for the ketones (Figure 14), it should be possible to use the plots shown in Figure 15 to predict ΔE_{rxn} values for a given deprotonated carbonyl species if the C=C occupancy has been determined by NBO analysis of the calculated (B3LYP/6-31G*) anionic structure. Furthermore, Figure 15 not only confirms the relative order of acidity among this series of carbonyl compounds to be imides > ketones > lactones > lactams, which is in line with the commonly accepted trend, but it also allows these differences in acidity to be quantified easily. The relatively high stability of imide-derived enolates, as indicated by Figure 15, may account for their low reactivity to a range of external nucleophiles.

To test the wider applicability of our computational approach to other carbonyl-containing functional groups, we next decided to analyze the bridgehead deprotonation of the diketopiperazines **117** and **118** performed by Williams et al. during their studies directed toward the total synthesis of bicyclomycin[5] (Scheme 19).

In their work, Williams et al. showed that the ratio of regioisomeric products obtained from deprotonation and subsequent electrophilic quench of **118** depended upon the length of time allowed between the deprotonation and quenching events (1 min and 1 h were typically used). The products of quenching from anion **122** were usually observed (in the presence of HMPA) when the electrophile was added 1 h after deprotonation, while the products derived from the anion **120** were observed (in the absence of HMPA) when the electrophile was added 1 min after deprotonation. This difference in behavior was attributed to anion **120** being the *kinetic* product of deprotonation and anion **122** being the *thermodynamic* product. Similar behavior was also observed for the homologous diketopiperazine **117**. As the magnitude of $J(^{13}C-H)$ coupling constants can be used to predict relative rates of deprotonation,[47] Williams was able to accurately predict that H_b ($J(^{13}C-H_b) = 167.9$ Hz **118** and 169.12 Hz **117**) would be kinetically more acidic than H_a ($J(^{13}C-H) = 143.9$ Hz **118** and 150.88 Hz **117**) in the [4.2.2] and [3.2.2] diketopiperazines respectively. Our computational analysis can now add a quantitative account of the *thermodynamic* acidity of H_a and H_b, as well as giving valuable insight into the structures the anions (i.e., are they enolate-like or carbanion-like character?). We therefore calculated ΔE_{rxn} for the deprotonation of both **117** and **118** and performed NBO analysis on the resulting anions **119**, **120**, **121** and **122** (Table 11).

The large negative calculated ΔE_{rxn} values clearly show that all four deprotonation reactions are highly favorable. Furthermore, there is a clear difference in stability between the two isomeric anions **119** and **121** derived from the [3.2.2]diketopiperazine **117** and also between the equivalent anions (**120** and **122**) derived from the [4.2.2]diketopiperazine **118**. In both cases it is the anion adjacent to the CH_2 in the bridge that is predicted to be most stable, and this is in complete agreement with the results obtained from the equilibration experiments performed by Williams et al. NBO analysis reveals that both anions (**119** and **121**) derived from the [3.2.2]diketopiperazine **117** are best described as α-keto carbanions, while the two anions (**120** and **122**) derived from the [4.2.2]diketopiperazine **118** are best described as enolate-like in nature. These results clearly show that simple generalizations cannot be made with regard to the nature of bridgehead-deprotonated species, even within the same family of compounds, and that calculations provide a valuable insight into their structure and behavior.

Conclusions

The viability of bridgehead lithiation-substitution of bridged carbonyl compounds has been tested in the laboratory, and we have demonstrated that lithiation-substitution is possible for ketones, lactones, lactams and imides having small bridges, including examples having [3.2.1], [3.2.2], [3.3.1], [4.2.1], and [4.3.1] skeletons. Smaller systems, where the sum of the bridging atoms (*S*) is 5, for example [2.2.1] or [3.1.1] ketones, or [2.2.1] lactams, did not undergo controlled bridgehead substitution. Ketones or lactams having a [2.2.2] structure also did not give bridgehead substitution. We have shown that B3LYP calculations accurately predict this difference in behavior with negative ΔE_{rxn} values being calculated for the successful deprotonations and positive ΔE_{rxn} values being calculated for the unsuccessful ones. NBO calculations were also performed on the anionic deprotonated species, and these show that some structures are best represented as bridgehead enolates and some are best represented as α-keto carbanions and that simple generalizations cannot be made with regard to their structure.

Acknowledgment. We thank the Engineering and Physical Sciences Research Council (EPSRC) for support of L.M. and J.B. through funding of a postdoctoral fellowship. We also thank the University of Nottingham, and GlaxoSmithKline, Stevenage, U.K., for support of D.T.K. through funding of a research studentship.

(47) Streitwieser, A., Jr.; Caldwell, R. A.; Young, W. R. *J. Am. Chem. Soc.* **1969**, *91*, 529.

Supporting Information Available: Full experimental procedures, characterization data and copies of ^{1}H and ^{13}C NMR spectra for all new compounds. A description of the computational methods used and details of all calculated structures (x,y,z coordinates, energies, zero point vibrational energies and frequencies). CIF files for all X-ray structures. Complete citations for refs 19 and 44. This material is available free of charge via the Internet at http://pubs.acs.org.

JA9009875